# The RING finger- and PDZ domain-containing protein PDZRN3 controls localization of the $Mg^{2+}$ regulator claudin-16 in renal tube epithelial cells

Received for publication, February 1, 2017, and in revised form, June 13, 2017 Published, Papers in Press, June 16, 2017, DOI 10.1074/jbc.M117.779405

**Kana Marunaka[‡], Chisa Furukawa[‡], Naoko Fujii[‡], Toru Kimura[§], Takumi Furuta[¶], Toshiyuki Matsunaga[‡], Satoshi Endo[‡], Hajime Hasegawa[‖], Naohiko Anzai[**], Yasuhiro Yamazaki[‡‡], Masahiko Yamaguchi[‡‡], and Akira Ikari[‡1]**

*From the [‡]Laboratory of Biochemistry, Department of Biopharmaceutical Sciences, Gifu Pharmaceutical University, Gifu 501-1196, [§]Department of Pharmacology and Toxicology, Kyorin University School of Medicine, Tokyo 181-8611, [¶]Institute for Chemical Research, Kyoto University, Kyoto 611-0011, [‖]Saitama Medical Center, Saitama Medical University, Saitama 350-8550, [**]Department of Pharmacology, Chiba University Graduate School of Medicine, Chiba 321-0293, and [‡‡]School of Pharmaceutical Sciences, University of Shizuoka, Shizuoka 422-8526, Japan*

Edited by Thomas Söllner

**Ion exchange in the renal tubules is fundamental to the maintenance of physiological ion levels. Claudin-16 (CLDN16) regulates the paracellular reabsorption of $Mg^{2+}$ in the thick ascending limb of Henle's loop in the kidney, with dephosphorylation of CLDN16 increasing its intracellular distribution and decreasing paracellular $Mg^{2+}$ permeability. CLDN16 is located in the tight junctions, but the mechanism regulating its localization is unclear. Using yeast two-hybrid systems, we found that CLDN16 binds to PDZRN3, a protein containing both RING-finger and PDZ domains. We also observed that the carboxyl terminus of the cytoplasmic CLDN16 region was required for PDZRN3 binding. PZDRN3 was mainly distributed in the cytosol of rat kidney cells and upon cell treatment with the protein kinase A inhibitor H-89, colocalized with CLDN16. H-89 also increased mono-ubiquitination and the association of CLDN16 with PDZRN3. Mono-ubiquitination levels of a K275A mutant were lower, and its association with PDZRN3 was reduced compared with wild-type (WT) CLDN16 and a K261A mutant, indicating that Lys-275 is the major ubiquitination site. An S217A mutant, a dephosphorylated form of CLDN16, localized to the cytosol along with PDZRN3 and the endosomal marker Rab7. PDZRN3 siRNA increased cell-surface localization of WT CLDN16 in H-89-treated cells or containing the S217A mutant and also suppressed CLDN16 endocytosis. Of note, H-89 decreased paracellular $Mg^{2+}$ flux in WT CLDN16 cells, and PDZRN3 siRNA increased $Mg^{2+}$ flux in the H-89-treated WT CLDN16 and S217A mutant cells. These results suggest that PDZRN3 mediates endocytosis of dephosphorylated CLDN16 and represents an important component of the CLDN16-trafficking machinery in the kidney.**

Cations and anions filtered in the renal glomeruli are reabsorbed in the renal tubules, which is divided into several segments. Each segment has different properties for reabsorption of ions. Filtered $Mg^{2+}$ is reabsorbed in the proximal tubule, thick ascending limb (TAL)[2] of Henle's loop, and distal tubule, and the percentages of reabsorption rate were ~30%, ~60%, and ~5%, respectively, and only 5% is excreted into the urine (1, 2). In the distal tubule, $Mg^{2+}$ is reabsorbed via a transcellular pathway. Transient receptor potential melastatin 6 channel is expressed in the apical membrane of the distal tubule and transports $Mg^{2+}$ from the lumen into the cells (3). Then, $Mg^{2+}$ may be transported by cyclin M2 from the cells to blood vessel (4). On the other hand, $Mg^{2+}$ is passively reabsorbed via a paracellular pathway dependent on the magnitude of a lumen-positive transepithelial potential difference in the TAL.

The permeability to ions via paracellular pathway is controlled by tight junctions (TJs). The TJ barrier contains aqueous channels capable of discriminating charge and molecular size, and its electrical resistance varies among different epithelia (5, 6). Claudins (CLDNs), a large family of transmembrane proteins, are major components of TJs and bear four transmembrane domains with cytoplasmic amino and carboxyl termini (7, 8). The carboxyl terminus of most CLDNs has a PDZ-binding motif that can interact with the PDZ domain of scaffolding proteins including zonula occludens 1 (ZO-1), ZO-2, and ZO-3. ZO-1 and ZO-2 indirectly link CLDNs to the actin cytoskeleton, and these junctional complexes are necessary to maintain the characteristics of permeability. Familial hypomagnesemia with hypercalciuria and nephrocalcinosis is a renal $Mg^{2+}$ and $Ca^{2+}$ wasting disorder caused by mutation in the *CLDN16* or *CLDN19* gene, resulting in impaired renal function and renal failure (9, 10). CLDN16 and CLDN19 can form homo- or hetero-oligomeric divalent cation-permeable pore and play a key role in the paracellular reabsorption of $Mg^{2+}$ in

This work was supported in part by JSPS KAKENHI Grant 15H04657 (to A. I.) and grants from the Salt Science Research Foundation (1627) and the Mishima Kaiun Memorial Foundation (to A. I.). The authors declare that they have no conflicts of interest with the contents of this article.

[1] To whom correspondence should be addressed: Laboratory of Biochemistry, Dept. of Biopharmaceutical Sciences, Gifu Pharmaceutical University, 1-25-4 Daigaku-nishi, Gifu 501-1196, Japan. Tel.: 81-58-230-8124; Fax: 81-58-230-8124; E-mail: ikari@gifu-pu.ac.jp.

[2] The abbreviations used are: TAL, thick ascending limb; TJ, tight junction; CLDN, claudin; H-89, *N*-[2-(*p*-bromocinnamylamino)ethyl]-5-isoquinolinesulfonamide; MDCK, Madin-Darby canine kidney; MESNA, sodium 2-mercaptoethanesulfonate; PDZRN, PDZ domain containing RING finger; TER, transepithelial electrical resistance; THP, Tamm-Horsfall glycoprotein; ZO, zonula occludens; EEA1, early endosomal antigen 1; Ub, ubiquitin.

the TJs of TAL (11). Various mutants of CLDN16 dissociate from the TJs and are distributed in the Golgi apparatus, endoplasmic reticulum, or lysosome (12–15). We previously reported that CLDN16 is dephosphorylated in Dahl salt-sensitive hypertensive rats (16) and the dephosphorylated mutant of CLDN16 is mainly distributed in the lysosome, resulting in little permeability to $Mg^{2+}$ (17). The mistargeting of CLDN16 must be a cause of hypomagnesemia; however, the regulatory mechanisms for trafficking of CLDN16 have not yet been clarified in detail.

PDZ domains are structural motifs that bind to a consensus motif at the carboxyl terminus of target proteins. A member of PDZ domain containing RING finger (PDZRN) includes a RING finger domain at an amino terminus and two or four PDZ domains at the carboxyl terminus. PDZRN3 has been reported to play positive roles in the myoblast differentiation (18) and nephrogenesis in *Xenopus laevis* (19). In contrast, it has negative roles in the bone morphogenetic protein-2-induced osteoblast differentiation (20) and adipogenesis in mouse 3T3-L1 preadipocytes (21). However, the functional characterization and binding target proteins of PDZRN3 have not been clarified in the mammalian kidney.

In the present study we investigated the novel association protein, which can regulate trafficking of CLDN16. In yeast two-hybrid systems, PDZRN3 was identified to bind to CLDN16. Immunofluorescence and immunoprecipitation assays showed that PDZRN3 is expressed in the CLDN16-expressing cells and binds to CLDN16 in the rat renal tubule. *N*-[2-(*p*-Bromocinnamylamino)ethyl]-5-isoquinolinesulfonamide (H-89), a protein kinase A (PKA) inhibitor, increased the association of CLND16 with PDZRN3 in Madin-Darby canine kidney (MDCK) cells expressing FLAG-tagged CLDN16. PDZRN3 siRNA suppressed endocytosis and increased the cell-surface expression of CLDN16 in the H-89-treated cells. Furthermore, PDZRN3 siRNA increased paracellular $Mg^{2+}$ flux from the apical to basal compartments. Similar results were observed in the cells expressing S217A mutant, a dephosphorylated form of CLDN16. Our present results indicate that PDZRN3 may be involved in the endocytosis of dephosphorylated CLDN16 from the TJs to intracellular compartments.

## Results

### *Association of CLDN16 with PDZRN3 in immunoprecipitation and pulldown assays*

To identify novel CLDN16-binding proteins involved in the regulation of its trafficking, we performed yeast two-hybrid screening using a human kidney cDNA library with the carboxyl cytoplasmic region of CLDN16 as bait. We obtained 234 positive clones and determined the sequences as described previously (22). Among them, we chose PDZRN3 (3 clones) as a candidate protein involved in regulating the trafficking of CLDN16 in the present studies. CLDN16 was previously shown to be exclusively expressed in the TAL of Henle's loop in humans (9), mice (23), and bovines (24). In the rat kidney, CLDN16 was localized in the cells expressing Tamm-Horsfall glycoprotein (THP), a marker of the TAL (Fig. 1*A*). PDZRN3 was widely expressed in the renal tubules including CLDN16-positive cells. These results indicate that PDZRN3 may be associated with CLDN16 in the kidney. To clarify the association between CLDN16 and PDZRN3, we performed immunoprecipitation assay using the homogenates from rat renal cortex. PDZRN3 was immunoprecipitated with anti-CLDN16 antibody but not with rabbit IgG (Fig. 1*B*). To clarify the binding site of CLDN16 with PDZRN3, we made a glutathione S-transferase (GST) fusion protein to the carboxyl cytoplasmic region of wild type (WT) and ΔPDZ mutant, a deletion form of the PDZ-binding motif (TRV at the carboxyl terminus) of CLDN16. In the pulldown assay, the WT CLDN16 was associated with PDZRN3, but ΔPDZ mutant was not (Fig. 1*C*). These results indicate that CLDN16 binds to PDZRN3 through the PDZ-binding motif.

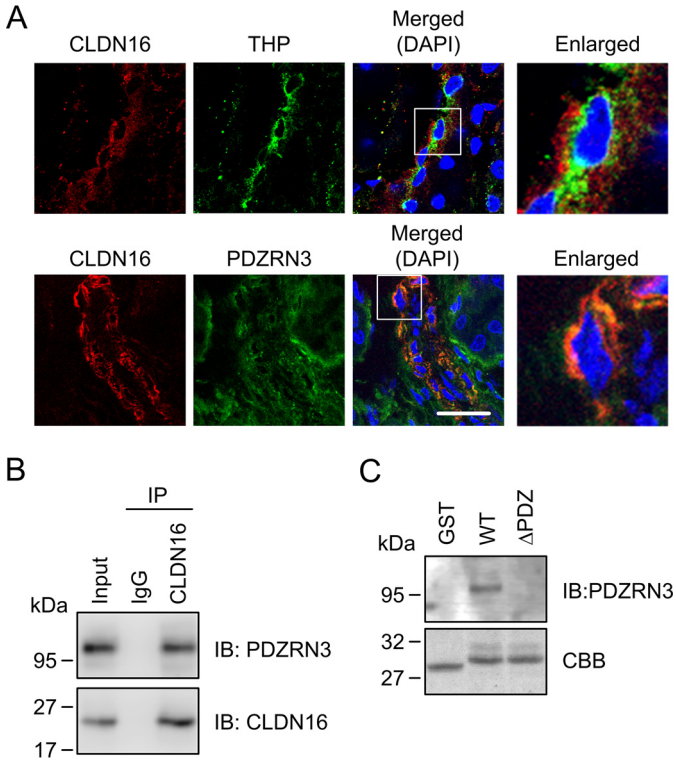


**Figure 1. Association of the carboxyl cytoplasmic region of CLDN16 with PDZRN3.** *A*, tissue sections were stained with anti-CLDN16 (*red*) plus anti-THP (*green*) or PDZRN3 (*green*) antibodies in the presence of DAPI (*blue*). The *right panels* show enlarged images of the *boxed area in the merged images*. The *scale bars* represent 10 μm. *B*, immunoprecipitation (*IP*) using control rabbit IgG and anti-CLDN16 antibodies were performed in the homogenates of rat renal cortex. The detergent extracts (input) and immune pellets were immunoblotted (*IB*) with anti-PDZRN3 and CLDN16 antibodies. *C*, the carboxyl cytoplasmic regions of WT or ΔPDZ mutant CLDN16 were fused with GST. GST, GST/WT-CLDN16, and GST/ΔPDZ-CLDN16 bound to glutathione-Sepharose beads were incubated with lysates of rat homogenates. Proteins on the beads were eluted with the sample buffer and immunoblotted with anti-PDZRN3 antibody or stained with Coomassie Brilliant Blue (*CBB*). The protein size marker is indicated on the left side. $n = 3–5$.

### *Effect of CLDN16 expression on the endogenous expression of junctional proteins*

We previously established stable cells expressing FLAG-tagged CLDN16 using MDCK/Tet-off cell line (25). The induction of CLDN16 by removal of doxycycline was confirmed by immunoblotting using anti-FLAG antibody (Fig. 2*A*). The expression levels of endogenous junctional protein including

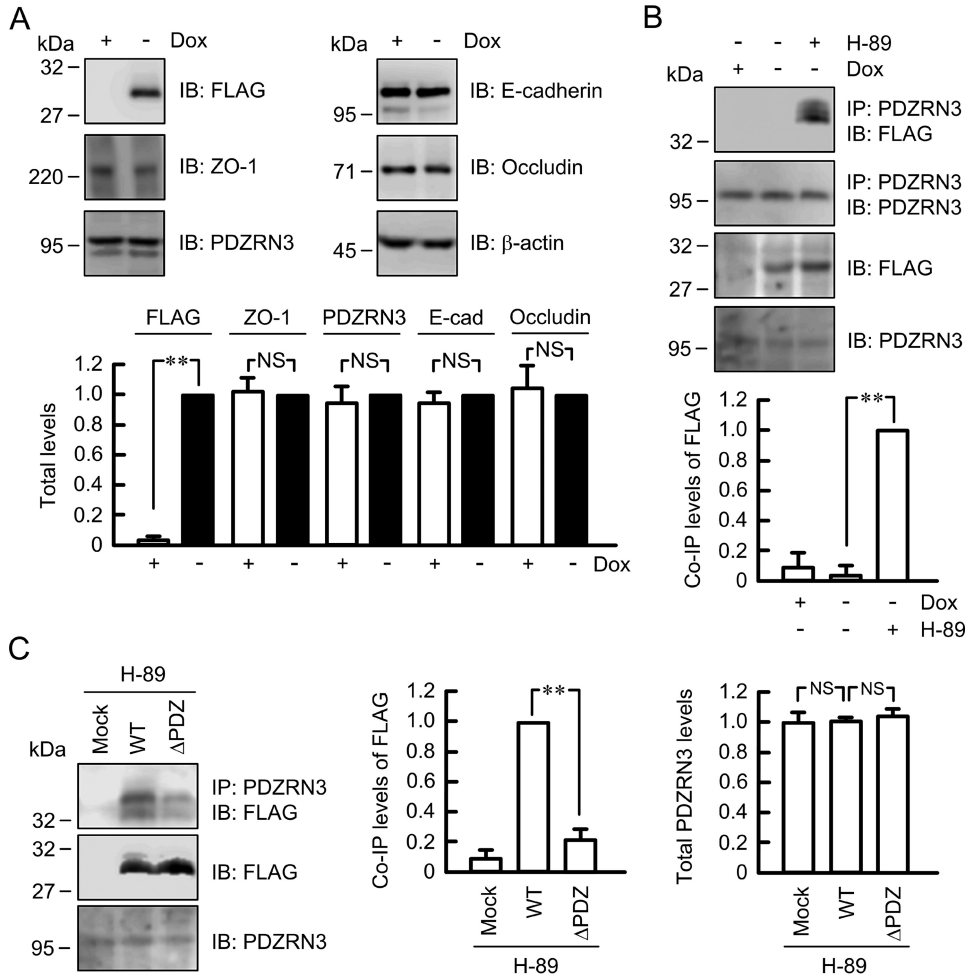


**Figure 2. Elevation of association between CLDN16 with PDZRN3 by H-89.** *A*, MDCK cells expressing FLAG-tagged CLDN16 were incubated in the presence and absence of 100 ng/ml doxycycline (*Dox*) for 72 h. Cell lysates were immunoblotted (*IB*) with anti-FLAG, ZO-1, PDZRN3, E-cadherin, occludin, and β-actin antibodies. The expression levels of each protein are represented as relative to the values in the absence of Dox. *B*, The cells were incubated in the presence and absence of 50 μM H-89 for 2 h. The cell lysates were immunoblotted with anti-FLAG and PDZRN3 antibodies. The cell lysates were immunoprecipitated with anti-PDZRN3 antibody. Immune pellets were immunoblotted with anti-FLAG or PDZRN3 antibody. Co-immunoprecipitated (*IP*) levels are represented as relative values of the bound FLAG-tagged CLDN16 with PDZRN3 in the cells treated with H-89 in the absence of Dox. *C*, MDCK cells were transiently transfected with mock, WT, or ΔPDZ-CLDN16 vector. At 48 h after transfection, the cell lysates were collected and immunoblotted with anti-FLAG and PDZRN3 antibodies. The cell lysates were immunoprecipitated with anti-PDZRN3 antibody, and immune pellets were immunoblotted with anti-FLAG antibody. Co-IP levels are represented as relative values of the bound FLAG-tagged CLDN16 with PDZRN3 in the cells expressing WT CLDN16. Total amounts of PDZRN3 are represented as relative to the values in the cells expressing WT CLDN16. $n = 3–4$. **, $p < 0.01$; *NS* (not significant), $p > 0.05$.

ZO-1, PDZRN3, E-cadherin, and occludin were not changed by CLDN16 expression. CLDN16 was not associated with PDZRN3 under control conditions, but H-89, a PKA inhibitor, increased the association between CLDN16 and PDZRN3 (Fig. 2*B*). The expression levels of PDZRN3 were not changed by the expression of mock, WT, and ΔPDZ mutant CLDN16 in the presence of H-89 (Fig. 2*C*). WT CLDN16 was associated with PDZRN3 in the presence of H-89, which was inhibited by the deletion of the PDZ-binding motif of CLDN16. These results indicate that the PDZ-binding motif within the carboxyl cytoplasmic region of CLDN16 is involved in the interaction with PDZRN3, consistent with the data of the pulldown assay.

### *Effects of H-89 and PDZRN3 siRNA on intracellular distribution of CLDN16*

Immunofluorescence assay showed that CLDN16 is colocalized with ZO-1 in the TJs, whereas it is not colocalized with Rab7, a late endosome marker, in the cytosol under control conditions (Fig. 3*A*). PDZRN3 was mainly distributed in the cytosol and slightly in the cell-cell contact area. H-89 increased the cytosolic distribution of CLDN16 and the colocalization of CLDN16 with PDZRN3 or Rab7 (Fig. 3, *B* and *F*). The colocalization of early endosomal antigen 1 (EEA1), an early endosome marker, with CLDN16 was slightly increased by H-89, whereas that with PDZRN3 was not (Fig. 3, *C* and *D*). The colocalization of CLDN16 with Rab7 caused by H-89 was inhibited by the introduction of PDZRN3 siRNA (Fig. 3, *E* and *F*). These results indicate that PDZRN3 may be involved in the regulation of intracellular trafficking of dephosphorylated CLDN16.

### *Effects of H-89 and PDZRN3 siRNA on ubiquitination and cell-surface localization of CLDN16*

Western blotting showed that the bands of FLAG-tagged CLDN16 are detected around 28 kDa in the short-exposure point (Fig. 4). In the long-exposure point, another band was detected around 36 kDa. The total levels of PDZRN3 and upper

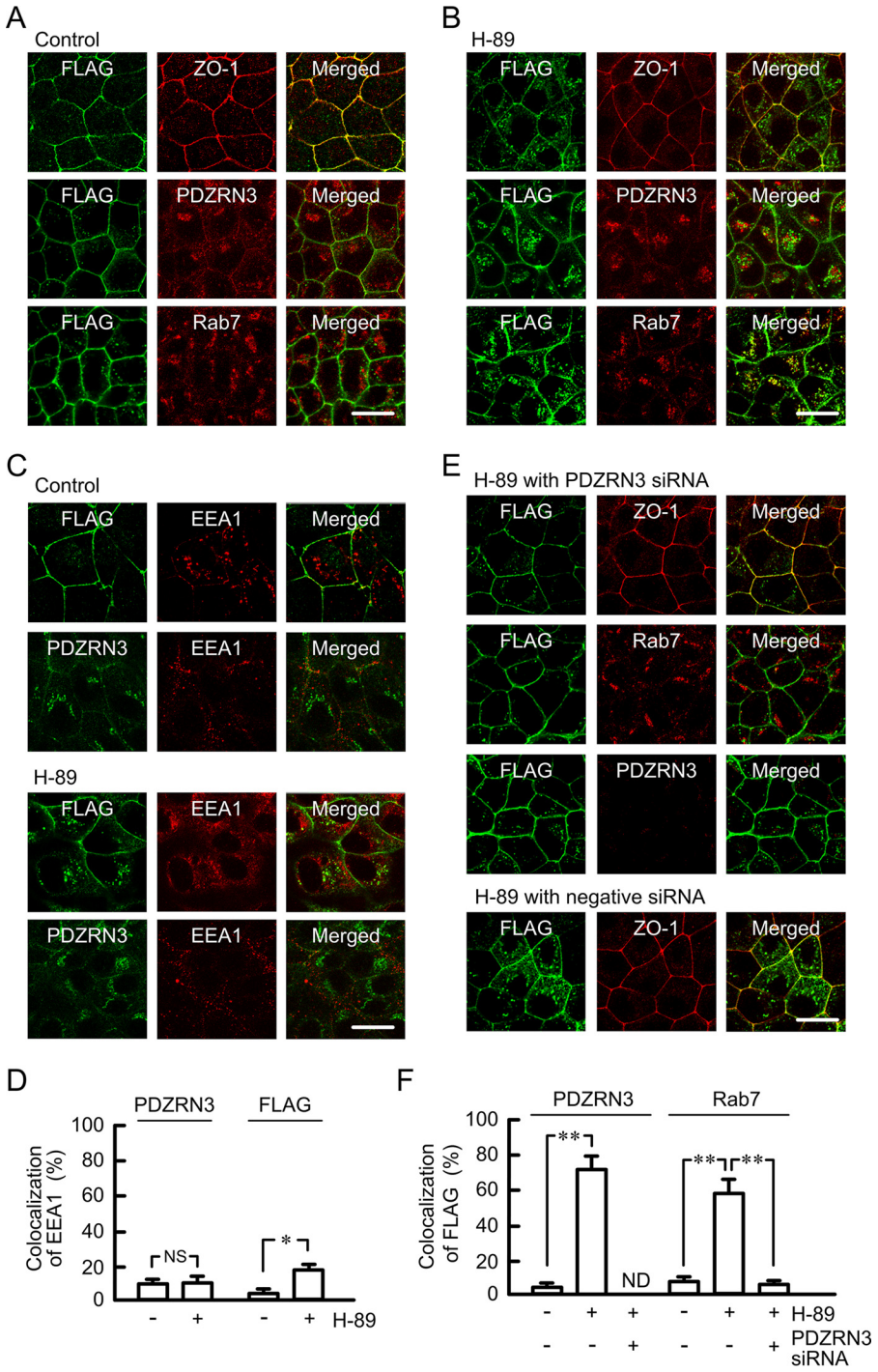


**Figure 3. Effects of H-89 and PDZRN3 siRNA on subcellular localization of CLDN16.** *A* and *B*, MDCK cells expressing FLAG-tagged WT CLDN16 were incubated in the presence and absence of 50 $\mu$M H-89 for 2 h. The cells were stained with anti-FLAG (CLDN16), ZO-1, PDZRN3, and Rab7 antibodies. *C*, cells were incubated in the presence and absence of 50 $\mu$M H-89 for 2 h. The cells were stained with anti-FLAG (CLDN16), PDZRN3, and EEA1 antibodies. *D*, the co-localization of PDZRN3 or CLDN16 with EEA1 were shown as the percentage ($n$ = 19–21 cells from >4 separate experiments). *E*, cells were transfected with negative control or PDZRN3 siRNA and then treated with H-89 for 2 h at 48 h after transfection. The cells were stained with anti-FLAG (CLDN16), ZO-1, PDZRN3, Rab7, and PDZRN3 antibodies. *F*, the co-localization of PDZRN3 or Rab7 with CLDN16 (FLAG) is shown as the percentage ($n$ = 24–48 cells from >4 separate experiments). The *scale bars* represent 10 $\mu$m. *ND* indicates not determined. **, $p < 0.01$; * $p < 0.05$; *NS* (not significant), $p > 0.05$.

bands of CLDN16 were decreased by the introduction of PDZRN3 siRNA, whereas those of CLDN1 and the lower bands of CLDN16 were not. The cell-surface biotinylation assay has been used to examine the cell-surface localization of CLDN1, CLDN2, and CLDN4 in MDCK cells (26–28). The level of cell-surface localization of CLDN16 in the H-89-treated cells was significantly lower than that in the control cells. PDZRN3 siRNA inhibited the H-89-induced reduction of cell-surface localization of CLDN16. In contrast, the cell-surface localization of CLDN1 was not changed by H-89 and PDZRN3 siRNA. Next, we examined the effect of PDZRN3 on ubiquitination of CLDN16. H-89 increased mono-ubiquitination level of

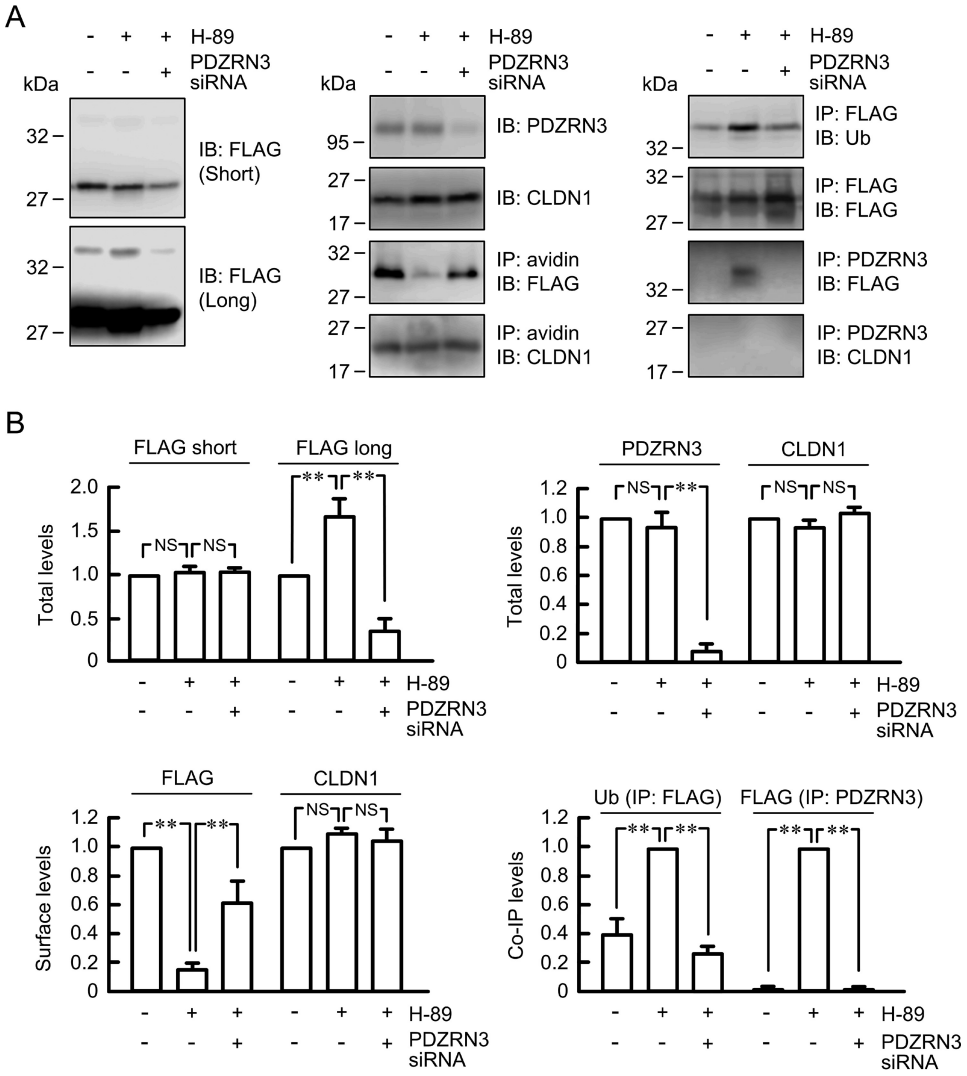


**Figure 4. Effects of H-89 and PDZRN3 siRNA on cell-surface localization and ubiquitination of CLDN16.** *A*, MDCK cells expressing FLAG-tagged WT CLDN16 were transfected with negative control or PDZRN3 siRNA. At 48 h after transfection, the cells were incubated in the presence and absence of 50 $\mu$M H-89 for 2 h. Total cell lysates were immunoblotted (*IB*) with anti-FLAG, PDZRN3, and CLDN1 antibodies. The chemiluminescent signals were detected at short or long exposure point (FLAG). The cell-surface proteins were labeled with biotin and immunoprecipitated with streptavidin-beads (*IP: avidin*). The immunoprecipitated proteins were immunoblotted with anti-FLAG and CLDN1 antibodies. Total cell lysates were immunoprecipitated with anti-FLAG or PDZRN3 antibodies. The immunoprecipitated proteins were immunoblotted with anti-ubiquitin (*Ub*), FLAG, and CLDN1 antibodies. *B*, total amounts of FLAG (short time, *lower band*), FLAG (long time, *upper band*), PDZRN3, and CLDN1 are represented as relative to the value in the cells without treatment of H-89 and PDZRN3 siRNA. Surface levels are represented as relative values of biotinylated CLDN16 and CLDN1 to the values in the cells without treatment of H-89 and PDZRN3 siRNA. Co-IP levels are represented as relative values of ubiquitinated CLDN16 and bound FLAG (CLDN16) with PDZRN3 to the values in the cells treated with H-89 in the absence of PDZRN3 siRNA. $n = 3$–4. **, $p < 0.01$ and *NS* (not significant), $p > 0.05$.

CLDN16 and the association of CLDN16 with PDZRN3, which were inhibited by the introduction of PDZRN3 siRNA. The bands of CLDN16 were detected around 36 kDa, which is similar to the size of ubiquitin-conjugated CLDN16. In contrast, CLDN1 was not associated with PDZRN3 in the control, H-89-treated, and PDZRN3 siRNA-transfected cells.

### *Ubiquitination of Lys-275 of CLDN16 by H-89*

Ubiquitination sites are predicted at Lys-261 and Lys-275 of human CLDN16 by the bioinformatics tool of CKSAAP_UbSite. Alanine substitution assay showed that the high molecular weight band of CLDN16 is decreased, and the low molecular weight band is increased by the mutation at K275A in the presence of H-89 (Fig. 5*A*). Total levels of PDZRN3 and CLDN16 were not changed by the mutation at K261A and K275A. The ubiquitination and association of PDZRN3 with CLDN16 were significantly inhibited by the mutation at Lys-275 but not at Lys-261 (Fig. 5*B*). These results indicate that Lys-275 of CLDN16 may be a major ubiquitination site.

### *Effect of PDZRN3 siRNA on endocytosis and stability of CLDN16 protein*

The association between CLDN16 and PDZRN3 may increase the trafficking of CLDN16 from the TJs to subcellular compartments. Therefore, we examined the effect of PDZRN3 siRNA on the endocytosis of CLDN16. CLDN16 was time-dependently internalized in the presence of H-89, which was suppressed by the knockdown of PDZRN3 (Fig. 6*A*). These results indicate that PDZRN3 may be involved in the endocytosis of dephosphorylated CLDN16 from the TJs to subcellular com-

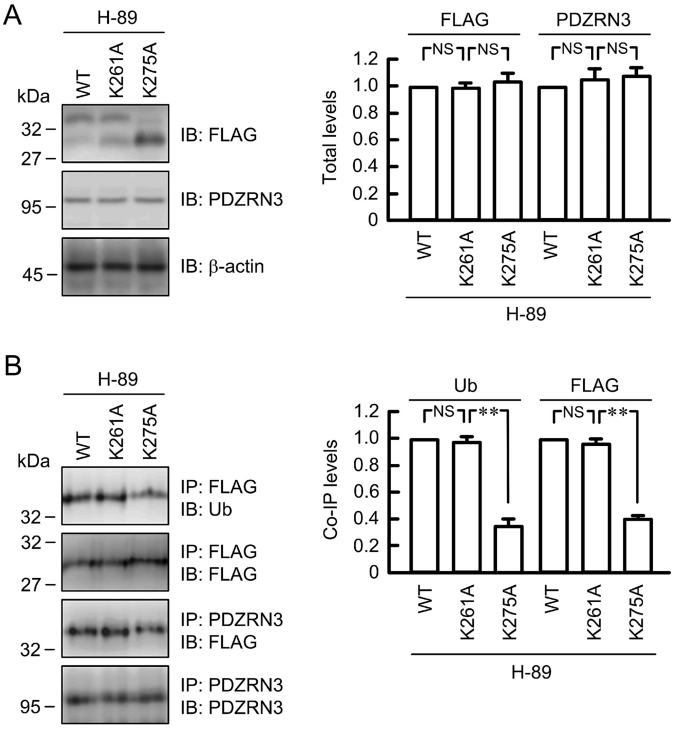


**Figure 5. Decrease in association between CLDN16 and PDZRN3 by mutation at Lys-275 of CLDN16.** MDCK cells were transfected with WT, K261A, or K275A mutant CLDN16. At 48 h after transfection, the cells were incubated in the presence and absence of 50 $\mu$M H-89 for 2 h. *A*, the cell lysates were immunoblotted (*IB*) with anti-FLAG, PDZRN3, and $\beta$-actin antibodies. Total levels of FLAG (high and low molecular weight bands) and PDZRN3 are represented as relative to the values in the cells transfected with WT CLDN16. *B*, the cell lysates were immunoprecipitated (*IP*) with anti-FLAG or PDZRN3 antibody. Immune pellets were immunoblotted with anti-Ub, FLAG, and PDZRN3 antibodies. Co-IP levels of ubiquitinated CLDN16 and bound FLAG (CLDN16) with PDZRN3 are represented as relative to the values in the cells transfected with WT CLDN16. $n = 3–4$. **, $p < 0.01$ and NS (not significant) $p > 0.05$.

partments. Next, we examined the effect of PDZRN3 on the protein stability of CLDN16. The levels of WT CLDN16 were time-dependently decreased in the presence of cycloheximide, an inhibitor of protein synthesis, and H-89 (Fig. 6*B*). The rate of decrease was significantly inhibited by the introduction of PDZRN3 siRNA. These results indicate that PDZRN3 has an effect on the protein stability of CLDN16 in the presence of H-89.

### *Effect of PDZRN3 siRNA on the intracellular localization and stability of S217A mutant CLDN16*

We previously reported that the tight junctional localization of CLDN16 is regulated by its phosphorylation at Ser-217 (17). S217A mutant, a dephosphorylated form of CLDN16, was mainly distributed in the cytosol and colocalized with PDZRN3 or Rab7 (Fig. 7, *A* and *C*). The association levels of CLDN16 with PDZRN3 and mono-ubiquitination of S217A mutant were higher than those of WT. In contrast, the level of cell-surface localization of S217A mutant was lower than that of WT. These results are similar to those in H-89-treated cells (Figs. 3 and 4). PDZRN3 siRNA increased the tight junctional localization of S217A mutant and colocalization between CLDN16 and ZO-1, whereas it decreased the co-localization between CLDN16 and Rab7 (Fig. 7, *B* and *C*). PDZRN3 siRNA increased the cell-surface localization of CLDN16, whereas it decreased mono-ubiquitination and the association with CLDN16. These results indicate that PDZRN3 is involved in the cytosolic retention of dephosphorylated CLDN16. Next, we examined the effect of PDZRN3 siRNA on the protein stability of S217A mutant CLDN16. The levels of S217A mutant CLDN16 were time-dependently decreased in the presence of cycloheximide, which were significantly inhibited by the introduction of PDZRN3 siRNA (Fig. 7*D*). These results are similar to those in the WT CLDN16-expressing cells treated with H-89.

### *Effect of PDZRN3 siRNA on paracellular permeability*

Induction of WT CLDN16 expression by removing doxycycline caused increases in transepithelial electrical resistance (TER) and paracellular $Mg^{2+}$ flux (Fig. 8, *A* and *B*). H-89 significantly inhibited the CLDN16-induced increase in TER and $Mg^{2+}$ flux, which was rescued by PDZRN3 siRNA. Similarly, TER and $Mg^{2+}$ flux were increased by PDZRN3 siRNA in the cells expressing S217A mutant CLDN16 (Fig. 8, *C* and *D*). These results indicate that dephosphorylation causes a loss of function of CLDN16 mediated by the mislocalization, which is rescued by PDZRN3 siRNA.

## Discussion

A dysfunction of CLDN16 or 19 is involved in the pathogenesis of hypomagnesemia. More than 40 and 10 mutations, respectively, have been currently identified in *CLDN16* and *CLDN19* genes (29). Mutations in *CLDN16* genes affect >28 different amino acids, which mainly occur in the extracellular loop and transmembrane domains. The mutants of CDLN16 distributed in the TJs have full or partial function after being transfected into LLC-$PK_1$ (15) and MDCK-C7 cells (12). In contrast, the mutants mislocalized to the intracellular compartments including the endoplasmic reticulum, Golgi apparatus, and lysosome lose their function. Therefore, the subcellular trafficking step of CLDN16 from intracellular compartments to the TJs plays an important role in the controlling $Mg^{2+}$ reabsorption under physiological conditions.

The intracellular localization of several CLDNs is regulated by phosphorylation. Phosphorylated CLDN1 and -2 are localized at the TJs in MDCK II cells (30, 31). CLDN4 phosphorylated by atypical protein kinase C (PKC) is localized at the TJs in human keratinocyte cells (32). Phosphorylation of CLDNs may be also involved in the pathogenesis. The phosphorylation status of CLDN4–7 was individually changed during the course of colitis caused by lipopolysaccharide in T84 colonic cells (33). Mislocalization of CLDN1 in the nuclei is caused by the PKC-dependent phosphorylation and increases metastasis in osteosarcoma cells (34). In contrast, nuclear localization of CLDN2 is increased by dephosphorylation and enhances proliferation in lung adenocarcinoma cells (35). Phosphorylation levels of CLDN16 in Dahl salt-sensitive hypertensive rats is lower than that in normotensive rats, and dephosphorylated CLDN16 caused by H-89 treatment is mainly distributed in the cytosol (16, 25). Furthermore, the elevation of extracellular $Mg^{2+}$ concentration increased the intracellular localization of CLDN16 mediated by the activation of the MEK/ERK pathway. The reg-

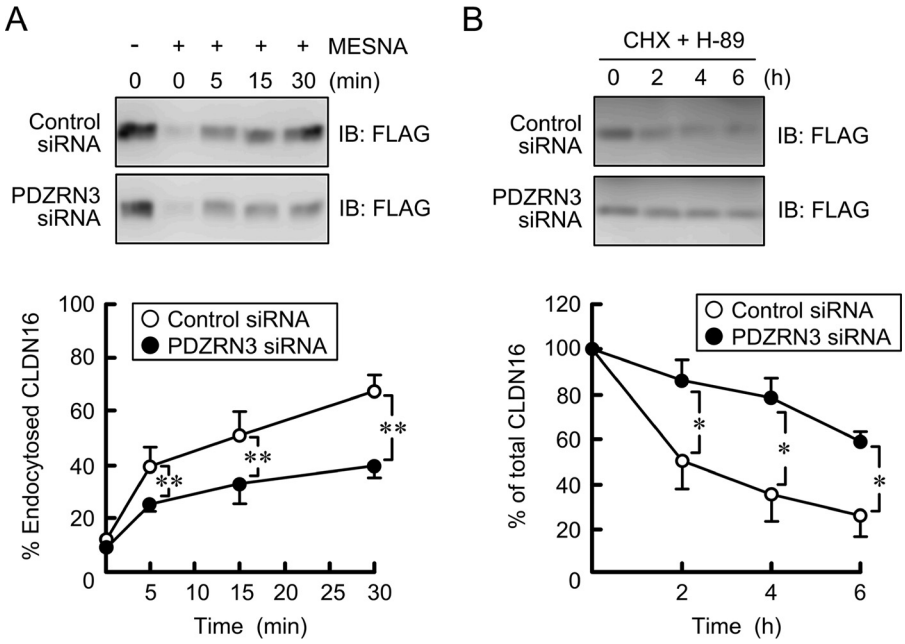


**Figure 6. Effect of PDZRN3 siRNA on endocytosis and stability of CLDN16 protein.** *A*, MDCK cells expressing FLAG-tagged WT CLDN16 were transfected with negative control or PDZRN3 siRNA. At 48 h after transfection, the cells were incubated in the presence and absence of 50 $\mu$M H-89 for 2 h. Plasma membrane proteins were biotinylated and then incubated for 0, 5, 15, and 30 min at 37 °C. Proteins remaining at the cell surface were stripped of biotin with MESNA. Internalized CLDN16 was collected and immunoblotted (*IB*) with anti-FLAG antibody. The band density of FLAG is represented as relative to the values in the absence of MESNA. *B*, the cells were transfected with negative control or PDZRN3 siRNA. At 48 h after transfection, the cells were incubated with 5 $\mu$M cycloheximide (*CHX*) plus 50 $\mu$M H-89 for the indicated periods. The cell lysates were immunoblotted with anti-FLAG antibody. The band density of FLAG is represented as relative to the values at 0 h. $n = 3$. **, $p < 0.01$; *, $p < 0.05$.

ulatory factors and the effect of phosphorylation on the localization of CLDNs may be different in each CLDN and tissue.

We recently reported that syntaxin-8, a target soluble *N*-ethylmaleimide-sensitive factor attachment protein receptor, binds to CLDN16 (22). The association of CLDN16 with syntaxin-8 and the cell-surface localization of CLDN16 are decreased by H-89 treatment. Furthermore, the association of S217A-mutant CLDN16 with syntaxin-8 is lower than that of WT, and the mutant was mainly localized in the cytosol. Therefore, we suggested that trafficking of CLDN16 from the intracellular compartments to the TJs is up-regulated by syntaxin-8. Here, we found that PDZRN3 binds to CLDN16 and the association of CLDN16 with PDZRN3 is increased by H-89 treatment. The endocytosis of CLDN16 was suppressed by PDZRN3 siRNA (Fig. 6*A*). These data indicate that the tight junctional localization of CLDN16 is inversely regulated by syntaxin-8 and PDZRN3. The late endosome marker Rab7 was colocalized with CLDN16 in the cells treated with H-89 or expressing S217A mutant. Therefore, we suggest that the endocytosis of dephosphorylated CLDN16 from the TJs to endosomes is up-regulated by PDZRN3. This is the first report showing that the intracellular trafficking of CLDNs is regulated by PDZRN3. Urinary cAMP excretion and the renal adenylate cyclase response to parathyroid hormone are lower in Dahl-salt-sensitive hypertensive rats than in Dahl-salt-resistant normotensive rats (36). Urinary $Mg^{2+}$ excretion is increased in hypertensive rats (37). We suggest that the reduction of cAMP content induces dephosphorylation of CLDN16 and PDZRN3-dependent endocytosis, resulting in the decrease in $Mg^{2+}$ reabsorption.

Four types of PDZRN (PDZRN1–4) have been cloned (38, 39), but the function of PDZRN3 and -4 is largely unknown. PDZRN2 (also known as ligand-of-Numb protein X1, LNX1) is a multidomain protein with E3 ubiquitin (Ub) ligase activity (40). Protein ubiquitination is mediated by three enzymes, Ub-activating (E1), Ub-conjugated (E2), and Ub-ligating (E3). E3 Ub ligases directly bind substrate and render substrate specificity. There are >600 putative E3 ligases with respect to individual protein substrates. Single or poly-Ub chain is covalently attached to lysine residues of target proteins. The Ub-interacting motifs are compiled into databases such as UbiProt, CKSAAP, and SysPTM. Using the CKSAAP database, we predicted the ubiquitination site of CLDN16 and found that Lys-275 is ubiquitinated by PDZRN3. PDZRN2 binds to junctional adhesion molecule (JAM4), a tight junctional one transmembrane protein, and regulates endocytosis of JAM4 (41). LNX1p80 binds to CLDN1 and induces endocytosis of CLDN1 in MDCK cells (42). An E3 Ub ligase complex Kelch-like 3 and Cullin 3 binds to CLDN8, resulting in ubiquitination and degradation of CLDN8 (43). Our data indicate that PDZRN3 binds to CLDN16 but not to CLDN1 (Fig. 4). We suggest that each CLDN can bind to different E3 Ub ligases. The E3 Ub ligase activity of PDZRN3 has not been investigated. In addition, PDZRN3 contains two PDZ domain, but it is unknown which domain is needed for the association with CLDN16. ZO-1 and ZO-2, which include three PDZ domains, are expressed in the TJ of TAL (44). We need further study to clarify the regulatory mechanism of tight junctional localization of CLDN16 by PDZ domain-containing proteins in the kidney.

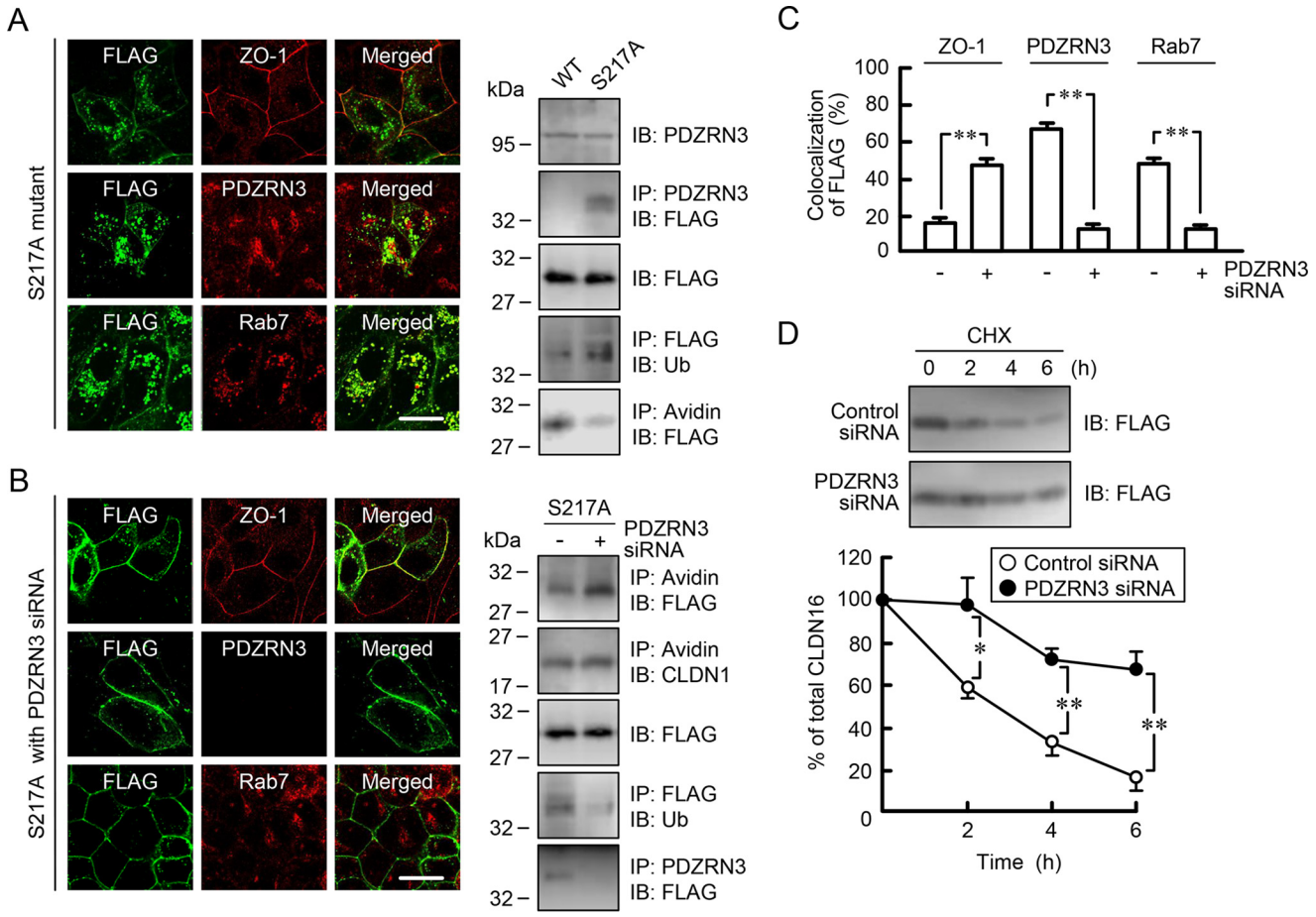


**Figure 7. Effect of PDZRN3 siRNA on the cell-surface localization and stability of S217A mutant CLDN16.** (*A*, *left images*) FLAG-tagged S217A mutant CLDN16 was stably expressed in MDCK cells. The cells were stained with anti-FLAG (CLDN16) plus anti-ZO-1, PDZRN3, or Rab7 antibodies. *A*, *right images*, the cell lysates were immunoblotted (*IB*) with anti-PDZRN3 and FLAG antibodies. After immunoprecipitation (*IP*) with anti-PDZRN3 or FLAG antibody, the immune pellets were immunoblotted with anti-FLAG or Ub antibody. The cell-surface-biotinylated proteins were precipitated using streptavidin-beads and immunoblotted with anti-FLAG antibody. *B*, *left images*, MDCK cells expressing FLAG-tagged S217A mutant CLDN16 was transfected with PDZRN3 siRNA. 48 h after transfection the cells were stained with anti-FLAG (CLDN16) plus anti-ZO-1, PDZRN3, or Rab7 antibodies. The *scale bar* represents 10 $\mu$m. *B*, *right images*, cell lysates were immunoblotted with anti-FLAG antibodies. The cell-surface-biotinylated proteins were precipitated using streptavidin-beads and immunoblotted with anti-FLAG or CLDN1 antibody. The cell lysates were immunoprecipitation with anti-PDZRN3 antibody, and the immune pellets were immunoblotted with anti-FLAG antibody. $n = 3–4$. *C*, the co-localization of CLDN16 (FLAG) with ZO-1, PDZRN3, or Rab7 is shown as the percentage ($n = 12–16$ cells from >3 separate experiments). *D*, the cells expressing S217A mutant CLDN16 were transfected with negative control or PDZRN3 siRNA. 48 h after transfection, the cells were incubated with 5 $\mu$M cycloheximide (*CHX*) for the indicated periods. The cell lysates were immunoblotted with anti-FLAG antibody. The band density of FLAG is represented as relative to the values at 0 h. $n = 3$. **, $p < 0.01$; *, $p < 0.05$.

The interaction between PDZ protein and target proteins is often regulated by phosphorylation of PDZ-binding motif. Phosphorylation of PDZ-binding motif down-regulates the interaction of the NR2B subunit of NMDA receptor with post-synaptic density 95 (PSD95) (45), membrane-associated guanylate kinase with corticotropin-releasing hormone receptor type 1 (46), GluR2 with GRIP1 (47), and Kir2.3 potassium channel with PSD95 (48). Canonical PDZ domains are composed of six $\beta$-strands ($\beta$A-$\beta$F) and two $\alpha$-helixes ($\alpha$A and $\alpha$B) (49). The Ser or Thr residue in the PDZ ligands may form hydrogen bonds with the side chain of the His residue at $\alpha$B-1 or $\alpha$B-5, respectively. Therefore, the phosphorylation of Ser or Thr residue may interfere with the interaction between these proteins (50). In contrast, phosphorylation of the PDZ-binding motif up-regulates the interaction of the myotilin and FATZ (calsarcin/myozenin) family proteins with ZASP/Cypher (51) and Yes-associated protein with Partitioning-defective 3 (52). Furthermore, dephosphorylation of PDZ-binding motif up-regulates the interaction of syndecan-1 with syntenin-1 (53). These reports indicate that the phosphorylation/dephosphorylation of PDZ-binding motif is involved in the interaction with target proteins. In contrast, there is no report showing that the PDZ-binding motif of CLDNs is phosphorylated. Interestingly, our data indicate that PDZRN3 binds to the PDZ-binding motif of CLDN16, and the interaction is up-regulated by the dephosphorylation of Ser-217, which is located at a different site from the PDZ-binding motif. The interaction between PDZRN3 and CLDN16 may be regulated by both the PDZ domain and the spatial structure near the phosphorylation site (Ser-217) of CLDN16.

Taken together, the results of the present study demonstrated that PDZRN3 directly binds to CLDN16 and is involved in the trafficking pathway of CLDN16 in renal tubular epithelial cells. This pathway was found to be sensitive to phosphorylation of CLDN16 at Ser-217 and mono-ubiquitination at Lys-275. Dephosphorylation of CLDN16 induced abnormal cyto-

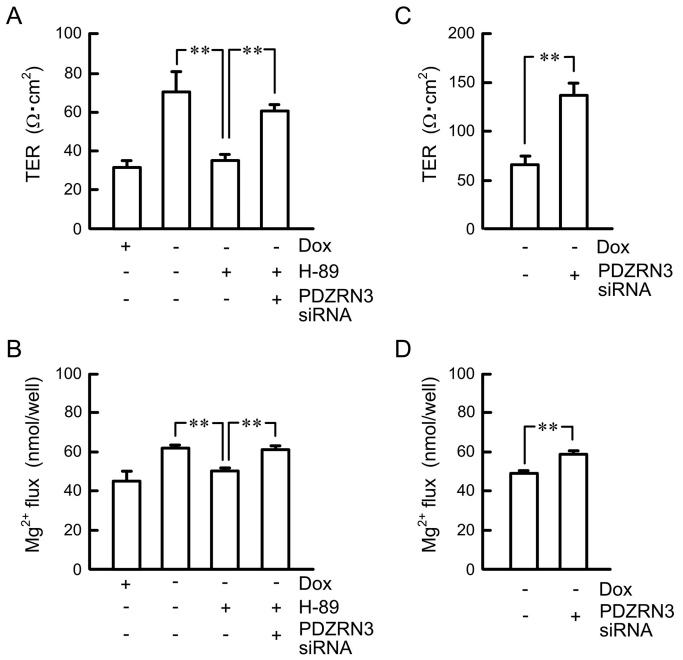


**Figure 8. Effects of H-89 and PDZRN3 siRNA on paracellular permeability.** MDCK cells expressing FLAG-tagged WT CLDN16 (*A* and *B*) or FLAG-tagged S217A mutant CLDN16 (*C* and *D*) were transfected with negative control or PDZRN3 siRNA and were cultured on transwell inserts for 72 h in the presence and absence of Dox. Then the cells were incubated with 50 $\mu$M H-89 for 2 h. *A* and *C*, TER was measured with a volt ohmmeter. *B* and *D*, transepithelial $Mg^{2+}$ permeability from the apical to basal compartment was measured using XB-1. $n = 4$. **, $p < 0.01$.

plasmic localization and loss of $Mg^{2+}$ transport, which were rescued by knockdown of PDZRN3. The physiological reabsorption of $Mg^{2+}$ in the TAL may be dynamically associated with the syntaxin 8- and PDZRN3-regulated expression of CLDN16 in the TJs.

## Experimental procedures

### *Materials*

Rabbit anti-ZO-1 antibody was obtained from Zymed Laboratories Inc. (South San Francisco, CA). Rabbit anti-FLAG antibody was from Medical & Biological Laboratories Co. (Nagoya, Japan). Mouse anti-FLAG antibody and sodium 2-mercaptoethanesulfonate (MESNA) were from Wako Pure Chemical Industries (Osaka, Japan). Rabbit anti-THP antibody was from Santa Cruz Biotechnology (Dallas, TX). Rabbit anti-Rab7 antibody was from Cell Signaling Technology (Beverly, MA). Rabbit anti-EEA1 antibody was from Affinity BioReagents (Golden, CO). H-89 was from LKT laboratories (St. Paul, MN). Lipofectamine 2000 was from Invitrogen. All other reagents were of the highest grade of purity available.

### *Yeast two-hybrid screening*

The interacting protein of carboxyl cytoplasmic region of CLDN16 was screened using the Matchmaker Gold Yeast Two-hybrid System (BD Biosciences Clontech, Mountain View, CA) as described previously (22).

### *Pulldown assay*

The carboxyl cytoplasmic region of human CLDN16 was subcloned into the pGEX4T1 vector (GE Healthcare). The vector was introduced into *Escherichia coli* BL21 and grown in the overnight express. GST-fused proteins were purified with glutathione-Sepharose 4B beads. The beads were incubated in buffer composed of 10 mM Tris-HCl (pH 7.5), 150 mM NaCl, 0.1% Nonidet P-40, 2 mM EDTA, 1 mM phenylmethylsulfonyl fluoride, and protease inhibitor mixture for 12 h at 4 °C. Bound proteins were then eluted with a sample buffer (2% SDS, 10% glycerol, 5% 2-mercaptoethanol, 0.2% bromphenol blue, and 0.2 mM Tris-HCl, pH6.8) and applied to the sodium dodecylsulfate (SDS)-polyacrylamide gel. Proteins were blotted onto a PVDF membrane and incubated with each primary antibody followed by a peroxidase-conjugated secondary antibody. The blots were visualized as described in the immunoblotting section.

**Table 1**
**Primers for PCR amplification and point mutation**

| Name | Direction | Sequence |
|---|---|---|
| CLDN16 | Forward | 5′-GATATCAATGAGGGATCTTCTTC-3′ |
| CLDN16 | Reverse | 5′-GTCGACTTACACCCTTGTGTCTAC-3′ |
| K261A | Forward | 5′-GCAGATGTTGGACCTGAGAGAAACTATC-3′ |
| K261A | Reverse | 5′-AAAAAGATATAAGCAGCAGGTGAGAAC-3′ |
| K275A | Forward | 5′-GCAGCCTATTCAGCCGCGGGTGTTTCC-3′ |
| K275A | Reverse | 5′-CCTCAAGGAATAAGGATAGTTTCTCTC-3′ |

### *Plasmid DNA construction*

Human CLDN16 cDNA was amplified by reverse transcriptase-polymerase chain reaction using a set of forward and reverse primers containing custom EcoRV and SalI restriction sites, respectively (Table 1). The cDNA was cloned into the mammalian expression vector, pCMV-Tag, containing the FLAG epitope, and subcloned into pTRE2hyg vector. The mutants of CLDN16 (K261A and K275A) were generated using a KOD-plus-mutagenesis kit (Toyobo Life Science, Osaka, Japan). Sequencing was performed by Bio Matrix Research (Chiba, Japan).

### *Cell culture and transfection*

The MDCK Tet-OFF cell line was obtained from BD Biosciences Clontech. Cells expressing FLAG-tagged WT and S217A mutant CLDN16 were generated previously (25). Cells were grown in Dulbecco's modified Eagle's medium (Sigma) supplemented with 5% fetal bovine serum, 0.07 mg/ml penicillin-G potassium, 0.14 mg/ml streptomycin sulfate, 0.1 mg/ml G418, and 0.1 mg/ml hygromycin B in a 5% $CO_2$ atmosphere at 37 °C. Plasmid DNA, PDZRN3 siRNA, and negative control siRNA (Sigma) were transfected into cells using Lipofectamine 2000 as recommended by the manufacturer.

### *Preparation of renal homogenates, cell lysates, and immunoprecipitation*

The homogenates of the rat renal cortex were prepared as described previously (16). Confluent MDCK cells were scraped into cold PBS and precipitated by centrifugation. The cells were then lysed in radioimmune precipitation assay buffer containing 150 mM NaCl, 0.5 mM EDTA, 1% Triton X-100, 50 mM Tris-HCl (pH 8.0), protease inhibitor mixture (Sigma), and 1 mM phenylmethylsulfonyl fluoride and were then sonicated for 20 s. After centrifugation at 1000 × *g* for 5 min, the supernatant

was collected (cell lysates). In the immunoprecipitation assay, cell lysates were incubated with protein G-Sepharose beads and anti-FLAG antibody at 4 °C for 16 h with gentle rocking. After centrifugation at 6000 × *g* for 1 min, the pellet was washed 3 times with the radioimmune precipitation assay buffer. In the biotinylation assay, cell-surface proteins were biotinylated as described previously (26). In the endocytosis assay, cell-surface proteins were biotinylated as described previously (26). After incubation of the cells for the period indicated, MESNA was used to cleave biotin from all cell-surface protein. The cell lysates, immunoprecipitants, and biotinylated proteins were solubilized in a sample buffer for SDS-polyacrylamide gel electrophoresis. Protein concentrations were measured by a protein assay kit (Bio-Rad) in which bovine serum albumin was used as a standard.

### SDS-polyacrylamide gel electrophoresis and immunoblotting

SDS-polyacrylamide gel electrophoresis was performed as described previously (54). Briefly, cell lysates or immunoprecipitates were applied to the SDS-polyacrylamide gel. Proteins were blotted onto a PVDF membrane and incubated with each primary antibody followed by a peroxidase-conjugated secondary antibody. Finally, the blots were incubated in EzWestLumi plus (ATTO Corp., Tokyo, Japan) and scanned with a C-DiGit Blot Scanner (LI-COR Biotechnology, Lincoln, NE). Band density was quantified with ImageJ software (National Institute of Health software). β-Actin was used for normalization.

### Measurement of TER and paracellular permeability

MDCK cells expressing FLAG-tagged CLDN16 were plated at confluent densities on transwells with polyester membrane inserts (Corning Inc.-Life Sciences, Acton, MA). TER was measured using Millicell-ERS volt-ohmmeter (Millipore, Bedford, MA). TER values (ohm·cm$^2$) were normalized by the area of the monolayer and calculated by subtracting the blank values (~35 ohm·cm$^2$) from the filter and bathing medium. Paracellular permeabilities to $Mg^{2+}$ were measured as described previously (55).

### Confocal microscopy

Rat kidney slices and MDCK cells expressing FLAG-tagged CLDN16 were immunostained as described previously (22). Immunolabeled cells were visualized on an LSM 700 confocal microscope (Carl Zeiss, Jena, Germany) set with a filter appropriate for DAPI, Alexa Fluor 488, and Alexa Fluor 546. Fluorescence intensities of CLDN16, Rab7, and PDZRN3 were determined by measuring the mean pixel density of staining area using ImageJ software (National Institute of Health, Bethesda, MD). The image area containing the signal from the TJ and cytosol was manually marked using ImageJ. After subtraction of background, the merged intensities of CLDN16 with PDZRN3 or Rab7 were shown as percentage of total intensities of CLDN16.

### Statistics

Results are presented as the mean ± S.E. Differences between groups were analyzed using one-way analysis of variance, and corrections for multiple comparisons were made using Tukey's multiple comparison test. Comparisons between two groups were made using Student's *t* test. Significant differences were assumed at $p < 0.05$.

*Author contributions*—K. M., C. F., and N. F. performed the experiments and analyzed the data. T. K., T. F., T. M., S. E., H. H., N. A., M. Y., and Y. Y. contributed to the experiment plan and discussion of the manuscript. A. I. contributed to supervision of the project, interpretation of the data, and writing the paper.

### References


1. Dai, L. J., Ritchie, G., Kerstan, D., Kang, H. S., Cole, D. E., and Quamme, G. A. (2001) Magnesium transport in the renal distal convoluted tubule. *Physiol. Rev.* **81,** 51–84
2. Konrad, M., Schlingmann, K. P., and Gudermann, T. (2004) Insights into the molecular nature of magnesium homeostasis. *Am. J. Physiol. Renal Physiol.* **286,** F599–F605
3. Schlingmann, K. P., Weber, S., Peters, M., Niemann Nejsum, L., Vitzthum, H., Klingel, K., Kratz, M., Haddad, E., Ristoff, E., Dinour, D., Syrrou, M., Nielsen, S., Sassen, M., Waldegger, S., *et al.* (2002) Hypomagnesemia with secondary hypocalcemia is caused by mutations in TRPM6, a new member of the TRPM gene family. *Nat. Genet.* **31,** 166–170
4. Stuiver, M., Lainez, S., Will, C., Terryn, S., Günzel, D., Debaix, H., Sommer, K., Kopplin, K., Thumfart, J., Kampik, N. B., Querfeld, U., Willnow, T. E., Němec, V., Wagner, C. A., Hoenderop, J. G., *et al.* (2011) CNNM2, encoding a basolateral protein required for renal $Mg^{2+}$ handling, is mutated in dominant hypomagnesemia. *Am. J. Hum. Genet.* **88,** 333–343
5. Powell, D. W. (1981) Barrier function of epithelia. *Am. J. Physiol.* **241,** G275–G288
6. Anderson, J. M., Van Itallie, C. M., and Fanning, A. S. (2004) Setting up a selective barrier at the apical junction complex. *Curr. Opin. Cell Biol.* **16,** 140–145
7. Morita, K., Furuse, M., Fujimoto, K., and Tsukita, S. (1999) Claudin multigene family encoding four-transmembrane domain protein components of tight junction strands. *Proc. Natl. Acad. Sci. U.S.A.* **96,** 511–516
8. Tsukita, S., Furuse, M., and Itoh, M. (2001) Multifunctional strands in tight junctions. *Nat. Rev. Mol. Cell Biol.* **2,** 285–293
9. Simon, D. B., Lu, Y., Choate, K. A., Velazquez, H., Al-Sabban, E., Praga, M., Casari, G., Bettinelli, A., Colussi, G., Rodriguez-Soriano, J., McCredie, D., Milford, D., Sanjad, S., and Lifton, R. P. (1999) Paracellin-1, a renal tight junction protein required for paracellular $Mg^{2+}$ resorption. *Science* **285,** 103–106
10. Konrad, M., Schaller, A., Seelow, D., Pandey, A. V., Waldegger, S., Lesslauer, A., Vitzthum, H., Suzuki, Y., Luk, J. M., Becker, C., Schlingmann, K. P., Schmid, M., Rodriguez-Soriano, J., Ariceta, G., Cano, F., *et al.* (2006) Mutations in the tight-junction gene claudin 19 (CLDN19) are associated with renal magnesium wasting, renal failure, and severe ocular involvement. *Am. J. Hum. Genet.* **79,** 949–957
11. Gong, Y., Renigunta, V., Zhou, Y., Sunq, A., Wang, J., Yang, J., Renigunta, A., Baker, L. A., and Hou, J. (2015) Biochemical and biophysical analyses of tight junction permeability made of claudin-16 and claudin-19 dimerization. *Mol. Biol. Cell* **26,** 4333–4346
12. Kausalya, P. J., Amasheh, S., Günzel, D., Wurps, H., Müller, D., Fromm, M., and Hunziker, W. (2006) Disease-associated mutations affect intracellular traffic and paracellular $Mg^{2+}$ transport function of Claudin-16. *J. Clin. Invest.* **116,** 878–891
13. Müller, D., Kausalya, P. J., Bockenhauer, D., Thumfart, J., Meij, I. C., Dillon, M. J., van't Hoff, W., and Hunziker, W. (2006) Unusual clinical presentation and possible rescue of a novel claudin-16 mutation. *J. Clin. Endocrinol. Metab.* **91,** 3076–3079
14. Konrad, M., Hou, J., Weber, S., Dötsch, J., Kari, J. A., Seeman, T., Kuwertz-Bröking, E., Peco-Antic, A., Tasic, V., Dittrich, K., Alshaya, H. O., von Vigier, R. O., Gallati, S., Goodenough, D. A., and Schaller, A. (2008) CLDN16 genotype predicts renal decline in familial hypomagnesemia with hypercalciuria and nephrocalcinosis. *J. Am. Soc. Nephrol.* **19,** 171–181
15. Hou, J., Paul, D. L., and Goodenough, D. A. (2005) Paracellin-1 and the modulation of ion selectivity of tight junctions. *J. Cell Sci.* **118,** 5109–5118

16. Ikari, A., Matsumoto, S., Harada, H., Takagi, K., Degawa, M., Takahashi, T., Sugatani, J., and Miwa, M. (2006) Dysfunction of paracellin-1 by dephosphorylation in Dahl salt-sensitive hypertensive rats. *J. Physiol. Sci.* **56,** 379–383
17. Ikari, A., Matsumoto, S., Harada, H., Takagi, K., Hayashi, H., Suzuki, Y., Degawa, M., and Miwa, M. (2006) Phosphorylation of paracellin-1 at Ser-217 by protein kinase A is essential for localization in tight junctions. *J. Cell Sci.* **119,** 1781–1789
18. Ko, J. A., Kimura, Y., Matsuura, K., Yamamoto, H., Gondo, T., and Inui, M. (2006) PDZRN3 (LNX3, SEMCAP3) is required for the differentiation of C2C12 myoblasts into myotubes. *J. Cell Sci.* **119,** 5106–5113
19. Marracci, S., Vangelisti, A., Raffa, V., Andreazzoli, M., and Dente, L. (2016) pdzrn3 is required for pronephros morphogenesis in *Xenopus laevis*. *Int. J. Dev. Biol.* **60,** 57–63
20. Honda, T., Yamamoto, H., Ishii, A., and Inui, M. (2010) PDZRN3 negatively regulates BMP-2-induced osteoblast differentiation through inhibition of Wnt signaling. *Mol. Biol. Cell* **21,** 3269–3277
21. Honda, T., Ishii, A., and Inui, M. (2013) Regulation of adipocyte differentiation of 3T3-L1 cells by PDZRN3. *Am. J. Physiol. Cell Physiol.* **304,** C1091–C1097
22. Ikari, A., Tonegawa, C., Sanada, A., Kimura, T., Sakai, H., Hayashi, H., Hasegawa, H., Yamaguchi, M., Yamazaki, Y., Endo, S., Matsunaga, T., and Sugatani, J. (2014) Tight junctional localization of claudin-16 is regulated by syntaxin 8 in renal tubular epithelial cells. *J. Biol. Chem.* **289,** 13112–13123
23. Hou, J., Shan, Q., Wang, T., Gomes, A. S., Yan, Q., Paul, D. L., Bleich, M., and Goodenough, D. A. (2007) Transgenic RNAi depletion of claudin-16 and the renal handling of magnesium. *J. Biol. Chem.* **282,** 17114–17122
24. Ohta, H., Adachi, H., Takiguchi, M., and Inaba, M. (2006) Restricted localization of claudin-16 at the tight junction in the thick ascending limb of Henle's loop together with claudins 3, 4, and 10 in bovine nephrons. *J. Vet. Med. Sci.* **68,** 453–463
25. Ikari, A., Ito, M., Okude, C., Sawada, H., Harada, H., Degawa, M., Sakai, H., Takahashi, T., Sugatani, J., and Miwa, M. (2008) Claudin-16 is directly phosphorylated by protein kinase A independently of a vasodilator-stimulated phosphoprotein-mediated pathway. *J. Cell Physiol.* **214,** 221–229
26. Ikari, A., Takiguchi, A., Atomi, K., and Sugatani, J. (2011) Epidermal growth factor increases clathrin-dependent endocytosis and degradation of claudin-2 protein in MDCK II cells. *J. Cell Physiol.* **226,** 2448–2456
27. Dukes, J. D., Whitley, P., and Chalmers, A. D. (2012) The PIKfyve inhibitor YM201636 blocks the continuous recycling of the tight junction proteins claudin-1 and claudin-2 in MDCK cells. *PLoS ONE* **7,** e28659
28. Angelow, S., and Yu, A. S. (2009) Structure-function studies of claudin extracellular domains by cysteine-scanning mutagenesis. *J. Biol. Chem.* **284,** 29205–29217
29. Günzel, D., Haisch, L., Pfaffenbach, S., Krug, S. M., Milatz, S., Amasheh, S., Hunziker, W., and Müller, D. (2009) Claudin function in the thick ascending limb of Henle's loop. *Ann. N.Y. Acad. Sci.* **1165,** 152–162
30. Fujii, N., Matsuo, Y., Matsunaga, T., Endo, S., Sakai, H., Yamaguchi, M., Yamazaki, Y., Sugatani, J., and Ikari, A. (2016) Hypotonic stress-induced down-regulation of claudin-1 and -2 mediated by dephosphorylation and clathrin-dependent endocytosis in renal tubular epithelial cells. *J. Biol. Chem.* **291,** 24787–24799
31. Van Itallie, C. M., Tietgens, A. J., LoGrande, K., Aponte, A., Gucek, M., and Anderson, J. M. (2012) Phosphorylation of claudin-2 on serine 208 promotes membrane retention and reduces trafficking to lysosomes. *J. Cell Sci.* **125,** 4902–4912
32. Aono, S., and Hirai, Y. (2008) Phosphorylation of claudin-4 is required for tight junction formation in a human keratinocyte cell line. *Exp. Cell Res.* **314,** 3326–3339
33. Li, J., Li, Y. X., Chen, M. H., Li, J., Du, J., Shen, B., and Xia, X. M. (2015) Changes in the phosphorylation of claudins during the course of experimental colitis. *Int. J. Clin. Exp. Pathol.* **8,** 12225–12233
34. Jian, Y., Chen, C., Li, B., and Tian, X. (2015) Delocalized claudin-1 promotes metastasis of human osteosarcoma cells. *Biochem. Biophys. Res. Commun.* **466,** 356–361
35. Ikari, A., Watanabe, R., Sato, T., Taga, S., Shimobaba, S., Yamaguchi, M., Yamazaki, Y., Endo, S., Matsunaga, T., and Sugatani, J. (2014) Nuclear distribution of claudin-2 increases cell proliferation in human lung adenocarcinoma cells. *Biochim. Biophys. Acta* **1843,** 2079–2088
36. Umemura, S., Smyth, D. D., Nicar, M., Rapp, J. P., and Pettinger, W. A. (1986) Altered calcium homeostasis in Dahl hypertensive rats: physiological and biochemical studies. *J. Hypertens.* **4,** 19–26
37. Wu, X., Ackermann, U., and Sonnenberg, H. (1995) Potassium depletion and salt-sensitive hypertension in Dahl rats: effect on calcium, magnesium, and phosphate excretions. *Clin. Exp. Hypertens.* **17,** 989–1008
38. Rice, D. S., Northcutt, G. M., and Kurschner, C. (2001) The Lnx family proteins function as molecular scaffolds for Numb family proteins. *Mol. Cell Neurosci.* **18,** 525–540
39. Katoh, M., and Katoh, M. (2004) Identification and characterization of PDZRN3 and PDZRN4 genes in silico. *Int. J. Mol. Med.* **13,** 607–613
40. Nie, J., McGill, M. A., Dermer, M., Dho, S. E., Wolting, C. D., and McGlade, C. J. (2002) LNX functions as a RING type E3 ubiquitin ligase that targets the cell fate determinant Numb for ubiquitin-dependent degradation. *EMBO J.* **21,** 93–102
41. Kansaku, A., Hirabayashi, S., Mori, H., Fujiwara, N., Kawata, A., Ikeda, M., Rokukawa, C., Kurihara, H., and Hata, Y. (2006) Ligand-of-Numb protein X is an endocytic scaffold for junctional adhesion molecule 4. *Oncogene* **25,** 5071–5084
42. Takahashi, S., Iwamoto, N., Sasaki, H., Ohashi, M., Oda, Y., Tsukita, S., and Furuse, M. (2009) The E3 ubiquitin ligase LNX1p80 promotes the removal of claudins from tight junctions in MDCK cells. *J. Cell Sci.* **122,** 985–994
43. Gong, Y., Wang, J., Yang, J., Gonzales, E., Perez, R., and Hou, J. (2015) KLHL3 regulates paracellular chloride transport in the kidney by ubiquitination of claudin-8. *Proc. Natl. Acad. Sci. U.S.A.* **112,** 4340–4345
44. Gonzalez-Mariscal, L., Namorado, M. C., Martin, D., Luna, J., Alarcon, L., Islas, S., Valencia, L., Muriel, P., Ponce, L., and Reyes, J. L. (2000) Tight junction proteins ZO-1, ZO-2, and occludin along isolated renal tubules. *Kidney Int.* **57,** 2386–2402
45. Chung, H. J., Huang, Y. H., Lau, L. F., and Huganir, R. L. (2004) Regulation of the NMDA receptor complex and trafficking by activity-dependent phosphorylation of the NR2B subunit PDZ ligand. *J. Neurosci.* **24,** 10248–10259
46. Bender, J., Engeholm, M., Ederer, M. S., Breu, J., Møller, T. C., Michalakis, S., Rasko, T., Wanker, E. E., Biel, M., Martinez, K. L., Wurst, W., and Deussing, J. M. (2015) Corticotropin-releasing hormone receptor type 1 (CRHR1) clustering with maguks is mediated via its C-terminal PDZ binding motif. *PLoS ONE* **10,** e0136768
47. Matsuda, S., Mikawa, S., and Hirai, H. (1999) Phosphorylation of serine-880 in GluR2 by protein kinase C prevents its C terminus from binding with glutamate receptor-interacting protein. *J. Neurochem.* **73,** 1765–1768
48. Cohen, N. A., Brenman, J. E., Snyder, S. H., and Bredt, D. S. (1996) Binding of the inward rectifier $K^+$ channel Kir 2.3 to PSD-95 is regulated by protein kinase A phosphorylation. *Neuron* **17,** 759–767
49. Lee, H. J., and Zheng, J. J. (2010) PDZ domains and their binding partners: structure, specificity, and modification. *Cell Commun. Signal.* **8,** 8
50. Jeleń, F., Oleksy, A., Smietana, K., and Otlewski, J. (2003) PDZ domains: common players in the cell signaling. *Acta Biochim. Pol.* **50,** 985–1017
51. von Nandelstadh, P., Ismail, M., Gardin, C., Suila, H., Zara, I., Belgrano, A., Valle, G., Carpen, O., and Faulkner, G. (2009) A class III PDZ binding motif in the myotilin and FATZ families binds enigma family proteins: a common link for Z-disc myopathies. *Mol. Cell Biol.* **29,** 822–834
52. Zhang, P., Wang, S., Wang, S., Qiao, J., Zhang, L., Zhang, Z., and Chen, Z. (2016) Dual function of partitioning-defective 3 in the regulation of YAP phosphorylation and activation. *Cell Discov.* **2,** 16021
53. Sulka, B., Lortat-Jacob, H., Terreux, R., Letourneur, F., and Rousselle, P. (2009) Tyrosine dephosphorylation of the syndecan-1 PDZ binding domain regulates syntenin-1 recruitment. *J. Biol. Chem.* **284,** 10659–10671
54. Ikari, A., Nakajima, K., Kawano, K., and Suketa, Y. (2001) Polyvalent cation-sensing mechanism increased $Na^+$-independent $Mg^{2+}$ transport in renal epithelial cells. *Biochem. Biophys. Res. Commun.* **287,** 671–674
55. Ikari, A., Hirai, N., Shiroma, M., Harada, H., Sakai, H., Hayashi, H., Suzuki, Y., Degawa, M., and Takagi, K. (2004) Association of paracellin-1 with ZO-1 augments the reabsorption of divalent cations in renal epithelial cells. *J. Biol. Chem.* **279,** 54826–54832